J Bioenerg Biomembr (2015) 47:395–408
DOI 10.1007/s10863-015-9624-x

Impairment of striatal mitochondrial function by acute paraquat poisoning

Analía Czerniczyniec[1] · E. M. Lanza[1] · A. G. Karadayian[1] · J. Bustamante[2] · S. Lores-Arnaiz[1]

Received: 27 March 2015 / Accepted: 31 August 2015 / Published online: 9 September 2015

Abstract Mitochondria are essential for survival. Their primary function is to support aerobic respiration and to provide energy for intracellular metabolic pathways. Paraquat is a redox cycling agent capable of generating reactive oxygen species. The aim of the present study was to evaluate changes in cortical and striatal mitochondrial function in an experimental model of acute paraquat toxicity and to compare if the brain areas and the molecular mechanisms involved were similar to those observed after chronic exposure. Sprague-Dawley rats received paraquat (25 mg/Kg i.p.) or saline and were sacrificed after 24 h. Paraquat treatment decreased complex I and IV activity by 37 and 21 % respectively in striatal mitochondria. Paraquat inhibited striatal state 4 and state 3 KCN-sensitive respiration by 80 % and 62 % respectively, indicating a direct effect on respiratory chain. An increase of 2.2 fold in state 4 and 2.3 fold in state 3 in KCN-insensitive respiration was observed in striatal mitochondria from paraquat animals, suggesting that paraquat redox cycling also consumed oxygen. Paraquat treatment increased hydrogen peroxide production (150 %), TBARS production (42 %) and cardiolipin oxidation/depletion (12 %) in striatal mitochondria. Also, changes in mitochondrial polarization was induced after paraquat treatment. However, no changes were observed in any of these parameters in cortical mitochondria from paraquat treated-animals. These results suggest that paraquat treatment induced a clear striatal mitochondrial dysfunction due to both paraquat redox cycling reactions and impairment of the mitochondrial electron transport, causing oxidative damage. As a consequence, mitochondrial dysfunction could probably lead to alterations in cellular bioenergetics.

Keywords Acute paraquat · Mitochondrial function · Oxygen consumption · Membrane potential

Abbreviations

$DiOC_6$	3, 3″-dihexyloxacarbocyanine iodide
EDTA	ethylenediaminetetraacetic acid
FCCP	carbonyl cyanide *p*-trifluoromethoxyphenylhydrazone
HRP	horseradish peroxidase
H_2O_2	hydrogen peroxide
NAO	acridine orange 10-nonyl bromide
SOD	superoxide dismutase
TBARS	thiobarbituric acid-reactive substances

Introduction

Paraquat (1,1'-dimethyl-4,4'-bipyridinium dichloride) is a highly toxic quaternary nitrogen herbicide. It is already known that chronic exposure of mice and rats to paraquat (10 mg/Kg) is associated with increased risk for neurodegenerative diseases, such as Parkinson's disease due to the selective degeneration of dopaminergic neurons of the substantia nigra (McCormack et al. 2002; Shimizu et al. 2003; Thiruchelvam et al. 2000). Previous work from our laboratory showed that chronic paraquat treatment induced cortical and striatal mitochondrial dysfunction and apoptosis (Czerniczyniec et al. 2011;

✉ Analía Czerniczyniec
aczerni@ffyb.uba.ar

[1] Instituto de Bioquímica y Medicina Molecular (UBA-CONICET), Facultad de Farmacia y Bioquímica, Universidad de Buenos Aires, Junín 956, C1113AAD Buenos Aires, Argentina

[2] Centro de Altos Estudios en Ciencias Humanas y de la Salud (CAECIHS), Facultad de Medicina, Universidad Abierta Interamericana, Buenos Aires, Argentina

Czerniczyniec et al. 2013). Deficient working conditions, improper maintenance, and climatic conditions make controlled and safe use of paraquat extremely difficult in developing countries. For this reason, human chronic exposure to paraquat (low doses during long time) is associated with rural workers. On the other hand, the biggest causes of acute poisoning are intentional self-poisoning or accidental ingestion. Approximately 68,000 cases of intoxication with paraquat have been reported per year around the world (Gram 1997; Sittipunt 2005). Also, it is liable for thousands of deaths from both voluntary and accidental ingestion (mortality rate more than 50 %) (Lin et al. 2014; Senarathna et al. 2009). In spite of its high toxicity, paraquat is registered and sold in around 90 developed and developing countries, including Argentina (Dinis-Oliveira et al. 2008; Paraquat information center 2015). The main target organ for acute paraquat toxicity is the lung as a consequence of its rapid accumulation in the type II epithelial cells of alveoli due to an active polyamine uptake transport system (Mainwaring et al. 2006). Paraquat has higher acute toxicity to humans than it does to rats. A large oral dose of PQ (>30 mg/kg in humans) rapidly leads to death from multi-organ failure (pulmonary edema, convulsions, cardiac, renal, and hepatic damage) (Agarwal et al. 2006; Agarwal et al. 2007; Onyeama and Oehme 1984). But, 16 mg/kg of paraquat may also lead to death through a progressive lung fibrosis and consequent respiratory failure after several days post-ingestion (Wesseling et al. 2001). In rats, after 24 h of a single intraperitoneal injection of paraquat (20–25 mg/kg), animals present symptoms of acute lung injury (Gocgeldi et al. 2008, Chen, 2001 #106; Mainwaring et al. 2006), that could be reversed by different pharmacological strategies such as treatment with oleanic acid (Santos et al. 2011), dexamethasone and melatonin (Gocgeldi et al. 2008) and sodium salicylate (Dinis-Oliveira et al. 2007).

Despite those numerous studies concerning acute paraquat-induced lung toxicity, the acute neurotoxicity of paraquat is poorly understood and remains important due to the fact that paraquat can cross blood-brain barrier (Shimizu et al. 2001). When paraquat is administered by ip injection (10 mg/Kg) to C57BL/6 J mice, 0.3 % of the dose enters the brain and it is then slowly eliminated (Breckenridge et al. 2013). The herbicide can accumulate in the striatum, frontal cortex, and cerebellum of C57BL/6 J mice (Prasad et al. 2007). Wu and collages (2013) recently described a slight damage to striatum, mesencephalon, frontal lobe and hippocampus 24 h after a single dose of paraquat (10.96 mg/kg body weight, i.p.). But then, 7 days later, the central nervous system is completely injured (Wu et al. 2013).

Taking into account that lung damage could be reversed by pharmacological treatment 1 or 2 h after acute paraquat poisoning, it would be important to know if a similar dose of the herbicide could also induce neurotoxicity. Due to the fact that mitochondria are essential for neuronal survival, the aim of the present study was to evaluate changes in cortical and striatal mitochondrial function in an experimental model of acute paraquat toxicity and to compare if the brain areas and the molecular mechanisms involved were similar to those observed after chronic exposure (Czerniczyniec et al. 2011; Czerniczyniec et al. 2013). Evaluation of mitochondrial function was achieved by different parameters, such as respiratory complexes activities, mitochondrial oxygen consumption, hydrogen peroxide (H_2O_2) production rates and mitochondrial membrane potential. Cardiolipin oxidation/depletion and TBARS were measured to evaluate the degree of lipid peroxidation and aconitase activity was determined as an index of protein oxidative damage.

Materials and methods

Animals

Sprague Dawley rats (all acquired from School of Pharmacy and Biochemistry) weighing 200–250 g at the beginning of experiments (ca. 2.5 months old) were kept in a soundproof room under a 12:12 h light/dark cycle photoperiod (lights on at 07.00 h) and controlled temperature (22 ± 2 °C). Food and water were available ad libitum. Measures were taken to minimize the animals' pain and discomfort, according to the principles and directives of the European Communities Council Directives (86/609/EEC) and according to the NIH Guide for the Care and Use of Laboratory Animals. They also received approval from the 6344/96 regulation of the Argentinean National Drug, Food and Medical Technology Administration (ANMAT) guidelines. Paraquat (1,1'-dimethyl-4,4'-bipyridinium dichloride) was dissolved in saline and administered at a dose of 25 mg/kg i.p. This dose of paraquat induced acute lung injury in rats and it corresponds to an acute non-occupational poisoning in humans (Gocgeldi et al. 2008; Mainwaring et al. 2006). Animals received saline or paraquat and were euthanized in a CO_2 chamber 24 h after the injection.

Isolation of mitochondria

Brains were quickly removed. Dissection was performed as described by Madison and Edison with some modifications (Madison and Edson 2001). Immediately after dissection, cerebral cortex and striatum from 3 control or paraquat-treated rats were pooled for each experimental group. Tissues were weighed and homogenized (1:5 *w*/*v*) in an ice-cold medium consisting of 0.23 M mannitol, 0.07 M sucrose, 5 mM Hepes and 1 mM EDTA, pH 7.4 (MSHE buffer). The homogenates were centrifuged at 700 *g* for 10 min to discard nuclei and cell debris. Then, the supernatant obtained was centrifuged at 8000 *g* for 10 min. The resulting pellet containing mitochondria was washed and resuspended in MSH buffer (0.23 M

mannitol, 0.07 M sucrose, 5 mM Hepes, pH 7.4) at a protein concentration of 20–25 mg/ml (Lores-Arnaiz et al. 1999). All the procedure was carried out at 0–4 °C. Mitochondrial samples were less than 2–4 % contaminated with cytosolic components according to the amount of lactate dehydrogenase present in the samples.

Protein content was assayed by using Folin phenol reagent and bovine serum albumin as standard (Lowry et al. 1951).

Mitochondrial respiratory complexes activity

NADH-cytochrome *c* reductase (Complex I-III) activity was measured in submitochondrial membranes by following spectrophotometrically the reduction of cytochrome *c* at 30 °C at 550 nm (ε = 19.6 $mM^{-1}cm^{-1}$) in a reaction medium containing 100 mM phosphate buffer (pH 7.4), 0.2 mM NADH, 25 μM cytochrome *c* and 0.5 mM KCN. Enzyme activity was expressed in nmol cytochrome *c* reduced/min/mg protein. Succinate cytochrome *c* reductase (Complex II-III) activity was similarly determined and expressed, except that NADH was substituted by 20 mM succinate.

Cytochrome oxidase activity (Complex IV) was assayed spectrophotometrically at 550 nm by following the rate of oxidation of reduced cytochrome *c* (Hatefi 1985). Cytochrome *c* was reduced with dithionite that was removed afterwards by eluting through a Sephadex-G25 column with potassium phosphate buffer (10 mM), pH 7.4. The reaction was initiated by the addition of 50 μM reduced cytochrome *c* to submitochondrial membranes (0.5 mg/ml) and the rate of reduced cytochrome *c* oxidation was determined as a pseudo-first-order reaction constant (*k*') [expressed as *k*'/mg protein].

Oxygen consumption

Oxygen uptake was determined in intact isolated mitochondria (0.5–1 mg/ml) with a two-channel respirometer for high-resolution respirometry (Oroboros Oxygraph, Paar KG, Graz, Austria). Mitochondrial respiratory rates were measured in a reaction medium containing 0.23 M mannitol, 0.07 M sucrose, 20 mM Tris-HCl (pH 7.4), 1 mM EDTA, 4 mM $MgCl_2$, 5 mM phosphate and 0.2 % bovine serum albumin at 30 °C. Malate (6 mM) and glutamate (6 mM) were used as substrates for Complex I to measure state 4 respiration and 1 mM ADP was added to measure state 3 respiration (Boveris et al. 1999). Oxygen uptake was expressed in ng-at O/min/mg protein. The respiratory control ratio (state 3 respiration/state 4 respiration) was determined in order to evaluate if isolation procedure or paraquat treatment affected mitochondrial physiology (Estabrook 1967).

In order to identify KCN-sensitive and -insensitive oxygen consumption rates, mitochondrial samples were incubated with 1.3 mM KCN. Then, we subtracted the rates of KCN-insensitive oxygen consumption rates (with KCN pre-incubation) to the original data (without KCN pre-incubation).

Also, respiratory rates were measured after incubation of mitochondrial samples with 1 μM DPI to evaluate the presence of paraquat redox cycling.

Hydrogen peroxide production

Hydrogen peroxide generation was determined in intact isolated mitochondria (0.1–0.3 mg/ml) by the scopoletin-HRP method, following the decrease in fluorescence intensity at 365–450 nm (λexc-λem) at 37 °C (Boveris 1984). The reaction medium consisted of 0.23 M mannitol, 0.07 M sucrose, 20 mM Tris-HCl (pH 7.4), 0.8 μM HRP, 1 μM scopoletin, 7 mM succinate, 6 mM glutamate and 0.3 μM SOD. This method allows the determination of H_2O_2 that diffuses from mitochondria to the buffer. Calibration was made using H_2O_2 (0.05–0.35 μM) as standard, in the presence and absence of catalase in order to express the fluorescence changes as nmol H_2O_2/min.mg protein.

Flow cytometry studies

Flow cytometry assays were performed in a FACScalibur (Becton-Dickinson) equipped with a 488 nm argon laser and a 615 nm red diode laser.

Population with high FSC (Forward Scatter) and SSC (Side Scatter) characteristics was chosen according to the typical mitochondrial size (3–5 μm) calibrated using Beads Calibrite (6 μm) (Becton Dickinson) for all the cytometric studies.

Mitochondrial membrane potential

Intact isolated mitochondria were loaded with 30 nM of the potentiometric cationic probe $DiOC_6$ during 20 min at 37 °C in MSH buffer (0.23 M mannitol, 0.07 M sucrose, 5 mM Hepes) supplemented with 5 mM malate, 5 mM glutamate and 1 mM phosphate. The procedure was carried out in a dark room (Bustamante et al. 2004). Mitochondrial fluorescence with no probe and after 0.5 μM FCCP (carbonyl cyanide p-trifluoromethoxyphenylhydrazone) treatment were used as negative and positive controls, respectively. In order to quantify the resulting fluorescence changes in the different mitochondrial samples, a common marker, indicating the relative fluorescence intensity of the respective mitochondrial population, was used.

Mitochondrial cardiolipin content

Acridine orange 10-nonyl bromide (nonyl acridine orange, NAO, λ_{em} 525 nm) binds specifically to cardiolipin molecule providing a direct and reliable method for evaluating the cardiolipin content in mitochondria (McMillin and Dowhan

2002; Petit et al. 1992; Wright et al. 2004) Nomura et al. (2000) reported that NAO is associated selectively with monolayer of cardiolipin. Also, they described that the binding of NAO to cardiolipin decreased by autoxidation. NAO is not able to bind peroxidated cardiolipin (CL-OOH) producing a decreased NAO fluorescence (Nomura et al. 2000). Previous observations indicate that low NAO fluorescence would be due to oxidation/depletion of cardiolipin (Nomura et al. 2000; Paradies et al. 2000; Paradies et al. 2001). This can be explained by the fact that free radicals-induced cardiolipin damage leads to decreased cardiolipin accessibility to NAO. Isolated cortical and striatal mitochondrial samples from control and paraquat-treated animals were loaded with 100 nM NAO during 20 min at 37 °C in MSH buffer supplemented with 5 mM malate, 5 mM glutamate and 1 mM phosphate. The procedure was carried out in a dark room. Then, mitochondria were acquired by the cytometer as previously described. Autofluorescence was also evaluated in samples without probe. Antimycin (0.5 μM), an inhibitor of the ubiquinone–cytochrome *c* reductase, was used as a positive control. We quantified the amount of events with high NAO fluorescence using a marker (M1), as a level of mitochondrial cardiolipin content (Czerniczyniec et al. 2013).

Thiobarbituric acid-reactive substances (TBARS) production

The amount of TBARS was determined by a fluorescence assay as described by Esterbauer et al. with some modifications (Esterbauer et al. 1982). Fresh isolated mitochondria were washed with 50 mM phosphate buffer (pH 7.4) in order to eliminate mannitol from the medium. Aliquots of mitochondrial samples were treated with 1 ml of 0.1 N sodium dodecyl sulphate, 1 ml of 0.1 N HCL, 0.15 ml of 10 % phosphotungstic acid and 0.5 ml of 0.7 % of 2-thiobarbituric acid. Butylated hydroxytoluene was added to a final concentration of 0.1 % (*w*/*v*). The mixture was heated in boiling water for 60 min. TBARS were extracted in 5 ml of n-butanol. After a brief centrifugation, the fluorescence of the butanolic layer was measured at 515 nm (excitation) and 553 nm (emission). The values were expressed as nmol of TBARS per milligram of protein, using a malondialdehyde standard prepared from 1,1,3,3-tetramethoxypropane.

Aconitase and fumarase activities

Aconitase and fumarase activities were measured in cortical and striatal mitochondrial samples from control and paraquat-treated animals using spectrophotometric rate determination (Gardner 2002). Freshly isolated mitochondria samples were sonicated (4 bursts of 30 s ON and 60 s OFF) followed by centrifugation at 8250 *g* for 10 min at 4 °C. Specific activity of the mitochondrial aconitase present in the supernatant was measured by monitoring the conversion of sodium citrate to α-ketoglutarate at 25 °C at 340 nm ($\varepsilon = 6.13\ mM^{-1}cm^{-1}$) using the coupled reduction of $NADP^+$ to NADPH by isocitrate dehydrogenase. The reaction medium contains 50 mM Tris-HCl buffer (pH 7.4), 0.6 mM $MnCl_2$, 5 mM sodium citrate, 0.2 mM $NADP^+$, 0.25 mg mitochondrial protein/ml and 1 U/ml isocitrate dehydrogenase. One milliunit of aconitase activity was defined as the amount of enzyme that catalyses the formation of 1 nmol of isocitrate/min (Gardner 2002). The specific activity of fumarase was subsequently determined by following spectrophotometrically the conversion of malate to fumarate at 240 nm in a reaction medium containing 50 mM phosphate buffer (pH 7.4), 0.25 mg mitochondrial protein/ml and 0.05 M sodium L-malate at 25 °C. The ratio of the specific activities of aconitase to fumarase was then calculated.

Drugs and chemicals

Paraquat (1,1'-dimethyl-4,4'-bipyridinium dichloride), ADP, BSA, EDTA, glutamic acid, HEPES, isocitrate dehydrogenase, $MnCl_2$, $NADP^+$, sodium citrate, malic acid, mannitol, scopoletin, HRP, succinate, sucrose, SOD, cytochrome *c*, Trizma base, FCCP and antimycin were purchased from Sigma Chemical Co (St. Louis, MO, USA). Other reagents were of analytical grade. NAO and $DiOC_6$ were purchased from Molecular Probes.

Statistical analysis

Results are presented as mean ± SEM. Prior to each analysis, test variables were checked for normality so all data were evaluated by the Kolmogorov-Smirnov test in order to follow a posterior parametric or nonparametric statistical analysis. Results were compared by unpaired independent Student's *t*-test in order to analyze the significance of differences between two groups. ANOVA followed by Tukey's test was used to analyze differences between mean values of more than two groups. SPSS (13.0 version) statistical software was used and a difference was considered to be statistically significant when $p < 0.05$.

Results

Mitochondrial respiratory complexes activity

Mitochondrial respiratory complex activities were measured in submitochondrial membranes from cerebral cortex and striatum of control and acute paraquat-treated rats. Figure 1a shows that paraquat treatment inhibited NADH-cytochrome *c* reductase activity by 37 % in striatal submitochondrial membranes ($p < 0.001$, as compared with control values), but no changes were observed in succinate-cytochrome *c* reductase

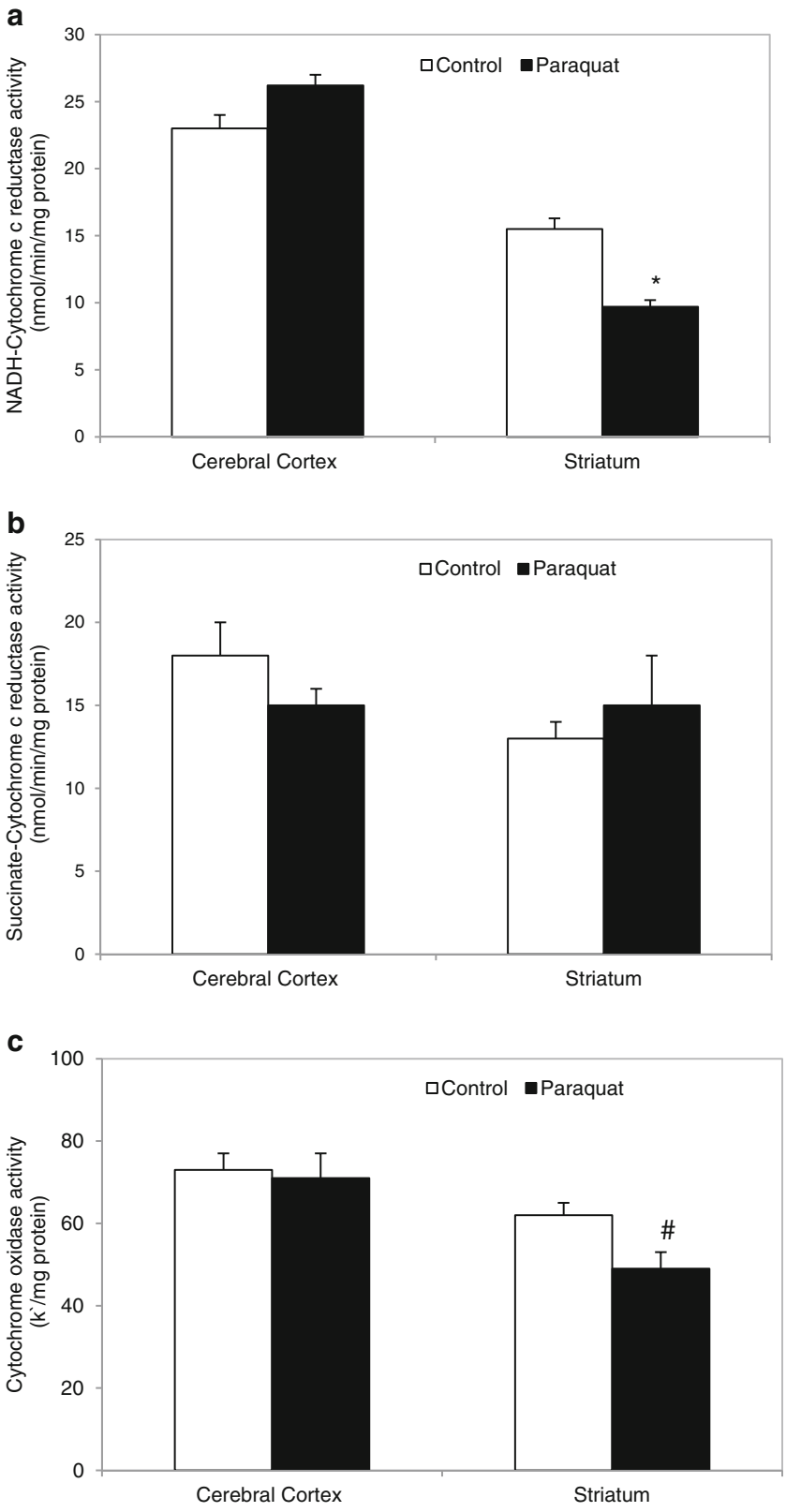

Fig. 1 Acute paraquat treatment effects on mitochondrial electron transfer activities. **(a)** *Complex I-III*, **(b)** *Complex II-III* y **(c)** *Complex IV*. Bars represent the mean ± SEM of 4 individual mitochondria samples, each obtained from a pool of cerebral cortex or striatum of 3 rats. (*$p < 0.001$; $^{\#}p < 0.05$ as compared with control value)

activity (Complex II-III) (Fig. 1b). Also, cytochrome oxidase (Complex IV) activity was decreased by 21 % in striatal sub-mitochondrial membranes from acute paraquat-treated rats ($p < 0.05$, as compared with control animals) (Fig. 1c). No significant changes were observed in cortical mitochondrial Complex I, II, III and IV activities.

Oxygen consumption

Malate-glutamate dependent oxygen consumption was measured in state 4 (at resting or controlled respiration) and in state 3 (active respiration, the maximal physiological rate of O_2 uptake and ATP synthesis). The respiratory control ratio (the most sensitive indicator of mitochondrial oxidative phosphorylation coupling) was calculated as the relationship between state 3/state 4 respiration rates.

Oxygen consumption rates of cortical and striatal intact mitochondria isolated from control and acute paraquat-treated animals are presented in Table 1. No significant changes were observed in state 4 and state 3 respiratory rates in cortical mitochondria from paraquat group, as compared to control animals. State 4 respiratory rates showed an increase of 40 % in striatal mitochondria from paraquat-treated animals ($p < 0.01$). However, acute paraquat treatment did not alter striatal oxygen consumption in state 3. Respiratory control of striatal mitochondria was significantly decreased, indicating the presence of an impaired respiratory function after acute paraquat treatment. In order to evaluate if the effects of paraquat on striatal oxygen consumption are related to paraquat redox cycling or a direct effect on respiratory complexes, mitochondria were pre-incubated with 1.3 mM KCN, a specific inhibitor of cytochrome oxidase. Using this strategy, we discriminated between KCN-sensitive and -insensitive oxygen consumption. As shown in Fig. 2a, paraquat inhibited striatal state 4 and state 3 KCN-sensitive respiration by 80 % and 62 % respectively, indicating a direct effect on respiratory chain. On the other hand, an increase of 2.2 fold in state 4 and 2.3 fold in state 3 in KCN-insensitive respiration was observed in striatal mitochondria from paraquat-treated animals, suggesting that paraquat redox cycling also consumed oxygen in a respiratory chain-independent manner (Fig. 2a).

In order to dilucidate the source of KCN-insensitive O_2 consumption, striatal mitochondrial samples were incubated with diphenylene iodonium (DPI), an inhibitor of NADPH oxidase 4 (NOX-4). Results are presented in Fig. 2b. No significant changes were observed in control O_2 consumption after 1 μM DPI pre-incubation. However, DPI inhibited by 81 and 76 % state 4 and state 3 KCN-insensitive respiration respectively, suggesting the involvement of paraquat redox cycling through NADPH oxidase.

Hydrogen peroxide production

Hydrogen peroxide production rates were determined in intact mitochondria isolated from control and acute paraquat-treated rats (Table 2). Hydrogen peroxide production was significantly increased by 150 % in striatal mitochondria from paraquat-treated animals ($p < 0.01$, as compared with control values). No significant changes were observed in H_2O_2 production of cortical mitochondria after acute paraquat treatment.

As described for oxygen consumption, striatal mitochondrial samples were pre-incubated with DPI. As shown in Table 2, 1 μM DPI inhibited striatal paraquat-induced H_2O_2 production by 43 %. No significant effects of DPI addition were observed on H_2O_2 production in striatal control mitochondria (Table 2).

Mitochondrial membrane potential

An important parameter of mitochondrial function is its transmembrane potential. Intact mitochondria isolated from different brain areas of control and paraquat-treated animals were used to determine the differences in $DiOC_6$ fluorescence by flow cytometry. The mitochondrial population and the autofluorescence level of unloaded samples are shown for cerebral cortex (a) and striatum (b) in Fig. 3. As described in the histograms, paraquat did not disturb cortical mitochondrial polarization (Fig. 3a). However, acute paraquat treatment induced an important increase in FL-1-$DiOC_6$ fluorescence in striatal mitochondria (Fig. 3b), indicating mitochondrial hyperpolarization. Quantification of $DiOC_6$ fluorescence in the different conditions is presented in Fig. 3c. Acute paraquat treatment significantly increased striatal mitochondrial membrane potential by 16 % ($p < 0.01$, as compared with control mitochondria). As expected, an important decrease in $\Delta\Psi_m$ was detected in mitochondria from both brain areas studied after 0.5 μM FCCP addition (positive control).

Table 1 Acute paraquat treatment effects on mitochondrial oxygen consumption

		Oxygen consumption (ng-at O/min/mg protein)		
		State 4	State 3	RC
Cerebral cortex	Control	21 ± 1	98 ± 5	4.6 ± 0.2
	Paraquat	20.9 ± 0.7	113 ± 7	5.3 ± 0.3
Striatum	Control	16.4 ± 0.9	73 ± 4	4.4 ± 0.2
	Paraquat	23 ± 1*	72 ± 4	3.1 ± 0.4#

Malate and glutamate were used as substrates. Values represent the mean ± SEM of 4–6 individual mitochondria samples, each obtained from a pool of cerebral cortex and striatum of 3 rats. (*$p < 0.01$; #$p < 0.05$, as compared with control value). RC: respiratory control index

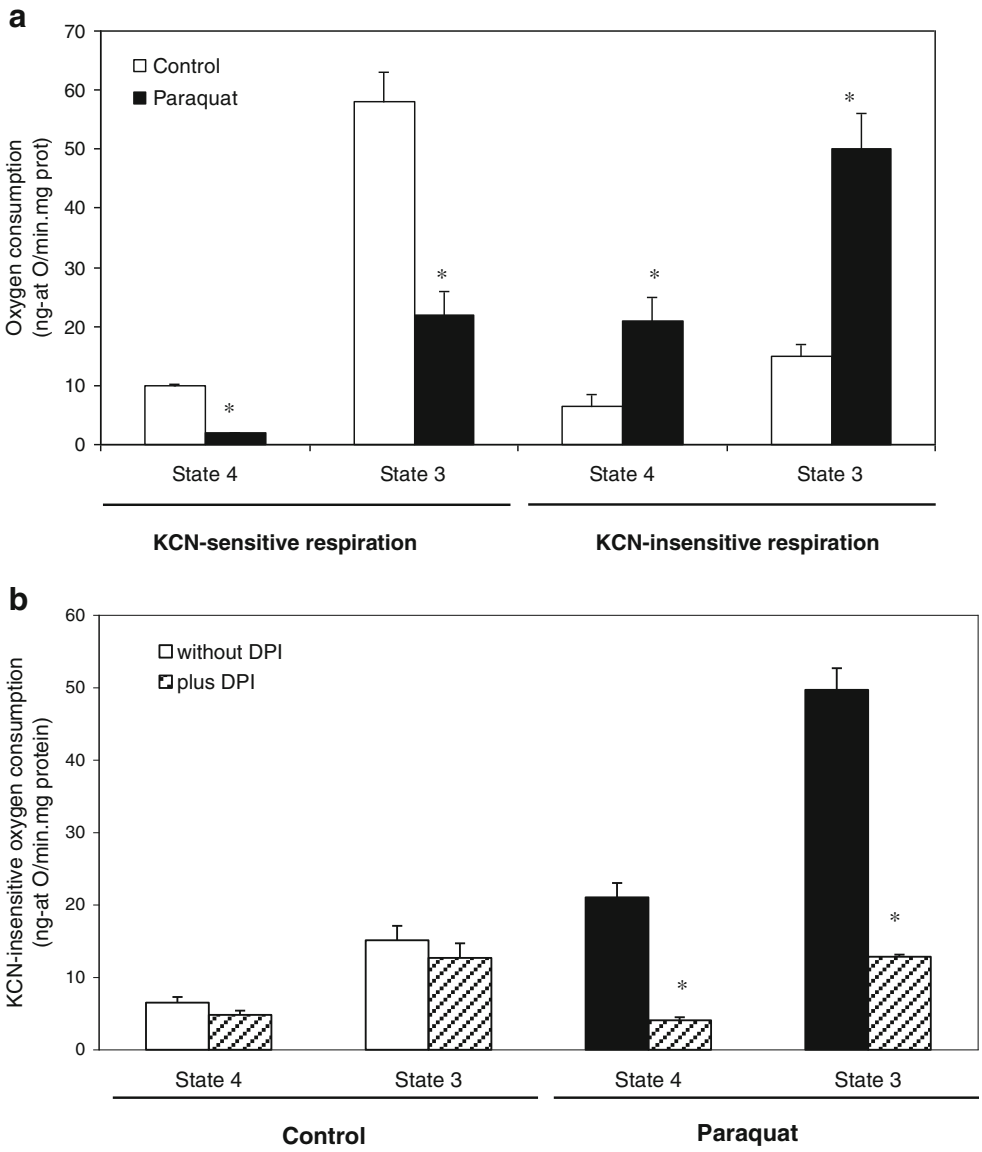

Fig. 2 Acute paraquat treatment effects on striatal mitochondrial oxygen consumption. **(a)** *Striatal KCN-sensitive and –insensitive oxygen consumption.* Malate and glutamate were used as substrates for State 4 and the same substrates plus 1 mM ADP for State 3 respiratory rates. Pre-incubation with 1.3 mM KCN renders KCN-insensitive respiration. Values represent the mean ± SEM of 4 individual mitochondria samples, each obtained from a pool of striatum of 3 rats. (*$p < 0.01$, as compared with its respective control value). **(b)** *DPI effect on striatal KCN-insensitive oxygen consumption.* Striatal mitochondrial samples were pre incubated with 1.3 mM KCN and with or without 1 μM DPI. Values represent the mean ± SEM of 4 individual mitochondria samples, each obtained from a pool of and striatum of 3 rats. (* $p < 0.001$, as compared with paraquat KCN-insensitive oxygen consumption)

Figure 4a, b illustrates ADP effects on membrane potential of striatal mitochondria from paraquat-treated and untreated (control) animals. Through overlay histograms of gated mitochondrial events (R1) we can observe that ADP addition to untreated striatal mitochondria (state 3 condition) induced as expected a 16 % decrease of membrane potential (Fig. 4c). ADP was able to induce in striatal mitochondria from paraquat-treated animals, a higher decrease (27 %) in mitochondrial membrane potential (Fig. 4c), that was not reverted by addition of 1 μM oligomycin (data not shown).

Table 2 Acute paraquat treatment effects on H_2O_2 production

	Hydrogen peroxide production (nmol H_2O_2/min/mg protein)	
	Control	Paraquat
Cerebral cortex	0.21 ± 0,07	0.23 ± 0.02
Striatum	0.16 ± 0.03	0.40 ± 0.04*
+ 1 μM DPI	0.13 ± 0.02	0.23 ± 0.01$^{\#,\dagger}$

Glutamate and succinate were used as substrates. Values represent the mean ± SEM of 4–6 individual mitochondria samples, each obtained from a pool of cerebral cortex or striatum of 3 rats. (*$p < 0.001$; $^{\#}p < 0.05$, as compared with control value; $^{\dagger}p < 0.01$, as compared with paraquat)

Cardiolipin content

Cortical and striatal mitochondria from control and acute paraquat-treated animals were analyzed for NAO staining by flow cytometry (Fig. 5). As described in the histograms, acute paraquat treatment did not alter NAO fluorescence in cortical mitochondria (Fig. 5a); although an important decrease in NAO fluorescence was induced in striatal mitochondria as

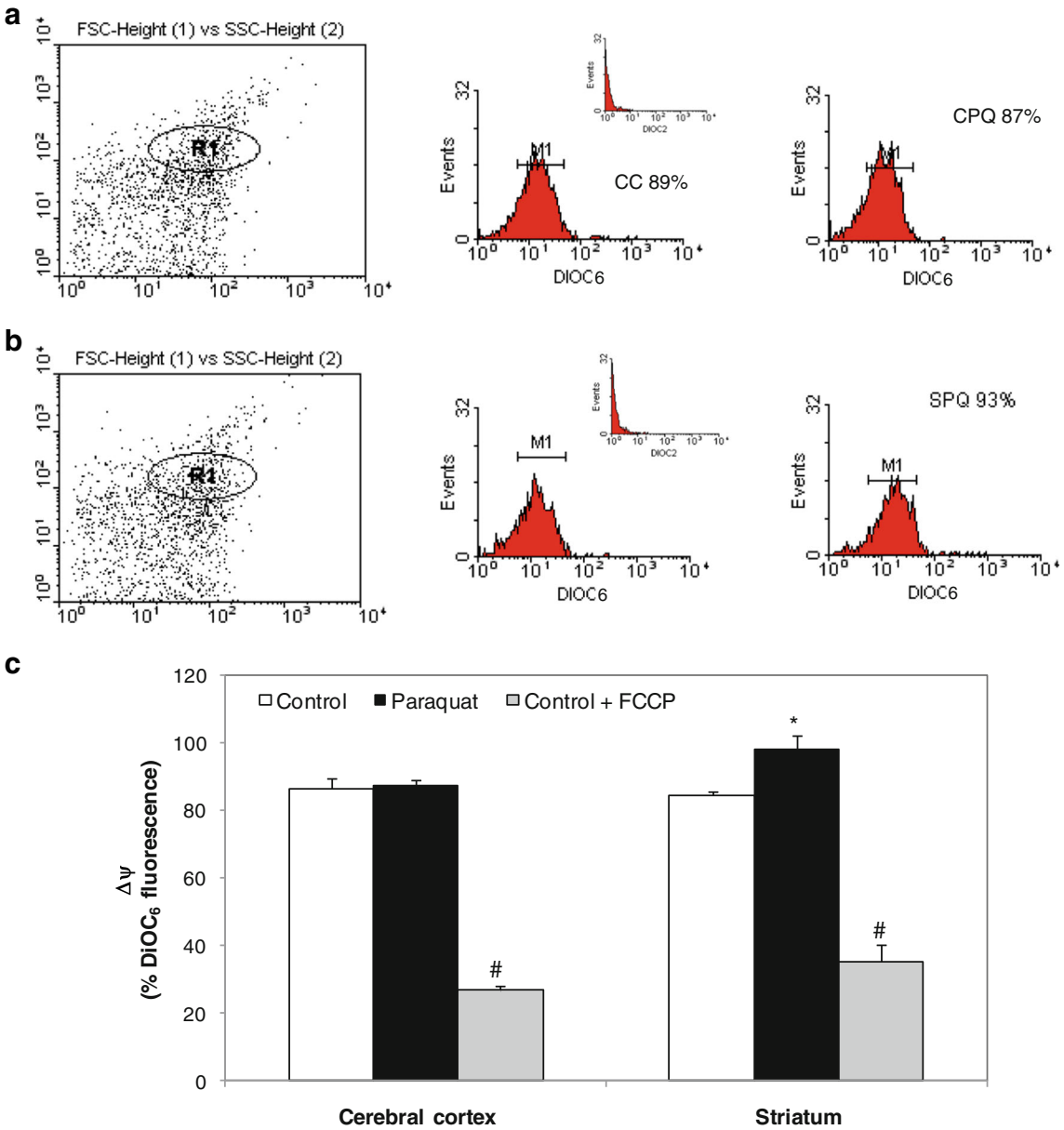

Fig. 3 Evaluation of mitochondrial membrane potential ($\Delta\Psi_m$). Mitochondrial membrane potential was measured in metabolic state 4 condition using malate and glutamate as substrates. Histograms of gated mitochondrial events (R1) versus relative fluorescence intensity (FL-1) from control and acute paraquat-treated animals were described: **(a)** Cerebral cortex and **(b)** Striatum. Each histogram represents a typical experiment out of three. CC: cerebral cortex-control animals, CPQ: cerebral cortex-paraquat treated animals, SC: striatum-control animals and SPQ: striatum-paraquat treated animals. Unloaded (no probe) mitochondria were included for the two groups (as inset). **(c)** Bars scheme of $DiOC_6$ fluorescence quantification corresponding to relative values of mitochondrial transmembrane potential. Bars represent the mean ± SEM of 3 different experiments. FCCP was used as positive control. (*$p < 0.01$ and $^{\#}p < 0.001$, as compared with its respective control value)

compared with control mitochondrial samples (Fig. 5b). Unloaded (no probe) mitochondria were included for the two groups (as inset). The difference in NAO fluorescence between the two groups, control and paraquat-treated animals was quantified under marker 1, for mitochondrial population with high cardiolipin content (Fig. 5c). As described in the histograms, no significant changes were observed in cardiolipin oxidation/depletion in cortical mitochondria from untreated and paraquat-treated animals. However, paraquat treatment decreased NAO relative fluorescence by 12 % ($p < 0.01$) in striatal mitochondria as compared with control mitochondria, indicating cardiolipin oxidation/depletion. As a positive control, antimycin (0.5 μM), an inhibitor of the ubiquinone-cytochrome *c* reductase was used. As expected, antimycin decreased basal cardiolipin levels in cortical mitochondria from control and paraquat-treated animals. In the

case of striatal mitochondria, antimycin only decreased cardiolipin levels in the control group but failed to induce changes in the paraquat-treated group of animals (Fig. 5c).

TBARS production

Thiobarbituric acid reactive substances are formed as a byproduct of lipid peroxidation. Paraquat treatment increased striatal TBARS production levels by 42 %, as compared with mitochondria from untreated animals (Fig. 6a). No significant changes were observed in TBARS production in cerebral cortex mitochondria after paraquat treatment.

Aconitase and fumarase activity

Mitochondrial aconitase activity is a functional indicator of oxidative damage to proteins, because its iron-sulfur core is frequently oxidized by superoxide anion, reducing the enzyme activity.

Activity of aconitase and fumarase was measured in mitochondria from control and paraquat-treated animals in the different brain areas. As shown in Fig. 6b, acute paraquat treatment did not affect aconitase/fumarase activity ratio in either cortical or striatal mitochondria.

Discussion

Several studies were carried out to evaluate the impact of chronic paraquat exposure in brain (McCormack et al. 2002; Ossowska et al. 2005) or to elucidate the effects of acute paraquat poisoning in lung (Dinis-Oliveira et al. 2007; Gocgeldi et al. 2008; Santos et al. 2011). However, very few studies have been made in reference to the effects of an acute dose of paraquat in the central nervous system. The present work was conducted in order to evaluate changes in cortical and striatal mitochondrial function after 24 h of an acute paraquat insult. Paraquat dose administered (25 mg/kg ip) was chosen in order to simulate an acute intoxication in humans, probably by self-poisoning or accidental ingestion. Due to the fact that in our chronic model of treatment cortical and striatal mitochondrial function is altered (Czerniczyniec et al. 2011), we decided to study the molecular mechanisms of acute paraquat neurotoxicity in the same brain areas in order to also compare the effect of different times of exposure.

Acute paraquat treatment induced important changes in mitochondrial oxygen consumption. Our results showed that acute paraquat treatment increased state 4 respiration in striatal mitochondria while state 3 does not seem to be affected. When we discriminated between KCN-sensitive and –insensitive oxygen consumption, we observed that paraquat decreased KCN-sensitive respiratory rates in both state 4 and state 3

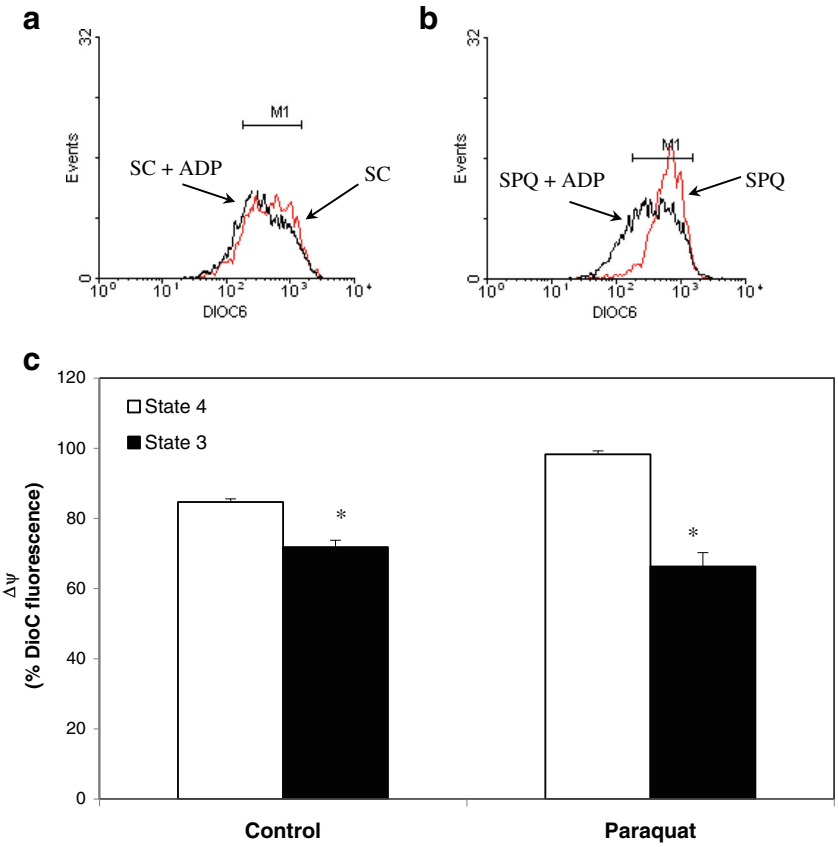

Fig. 4 ADP effect on striatal mitochondrial membrane potential ($\Delta\Psi_m$). Mitochondrial membrane potential from striatal untreated (control) and paraquat treated animals was measured in metabolic state 4 (malate-glutamate) and in state 3 (malate-glutamate plus 1 mM ADP). Overlay histograms of gated mitochondrial events (R1) versus relative fluorescence intensity (FL-1) from control **(a)** and acute paraquat-treated animals **(b)** represents a typical experiment out of three. SC: striatum-control animals and SPQ: striatum-paraquat treated animals. **(c)** Bars scheme of $DiOC_6$ fluorescence quantification corresponding to relative values of mitochondrial transmembrane potential. Bars represent the mean ± SEM of 3 different experiments. (*$p < 0.05$, as compared with its respective control value)

probably as a consequence of the inhibition of respiratory complex I and complex IV (Fig. 1). On the contrary, paraquat significantly increased KCN-insensitive oxygen consumption, probably through paraquat redox cycling reactions. It is well known that paraquat undergoes redox cycling being reduced by diaphorases, such as NADPH oxidase (NOX). This point was evaluated in our experimental model through the pre-incubation of mitochondrial samples with diphenylene iodonium (DPI), an inhibitor of NADPH oxidase activity. It has been recently described that NOX-4 is localized in the mitochondria of rat kidney cortex (Block et al. 2009), cardiac myocites (Case et al. 2013; Kuroda et al. 2010) and PC12 cells (Huang et al. 2015). As shown in Fig. 2, DPI decreased striatal KCN-insensitive respiration in mitochondria from paraquat-treated animals in both state 4 and state 3, suggesting that paraquat is still present in mitochondria and also is reduced by NOX-4 consuming oxygen independently of respiratory chain activity. Summing up, electron transport chain (KCN-sensitive respiration) and mitochondrial paraquat oxidative reactions by NOX-4 (KCN-insensitive respiration) seem to

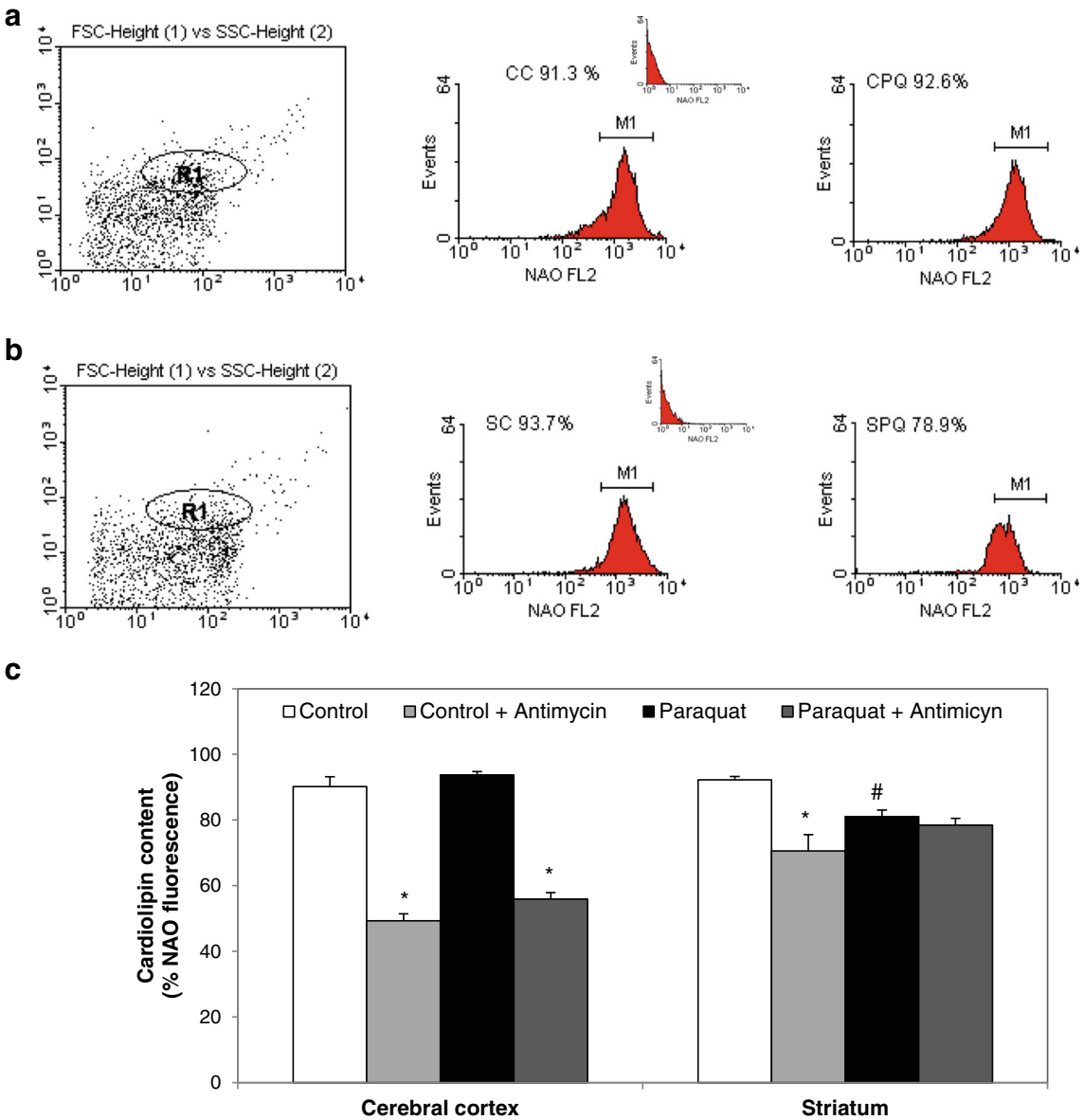

Fig. 5 Effects of paraquat treatment on NAO fluorescence. Fluorescence histograms (FL-2) of cortical **(a)** and striatal **(b)** mitochondrial events from control and paraquat-treated animals. Autofluorescence was evaluated without probe (inset). CC: cerebral cortex from control animals, CPQ: cerebral cortex from paraquat-treated animals. SC: striatum from control animals and SPQ: striatum from paraquat-treated animals. Each histogram represents a typical experiment out of three. **(c)** Bars graph quantification of the amount of events with high NAO relative fluorescence was conducted using a marker (M1), indicative of the level of cardiolipin content. Bars represent the mean ± SEM of 3 different experiments. Antimycin A was used as positive control of lipid peroxidation. (*$p < 0.01$ and $^{\#}p < 0.05$ as compared with its respective control value)

compete for all the oxygen available and mainly required for ATP synthesis and necessary for neurons survival.

The inhibition of complex I activity and the redox cycling reactions due to the residual paraquat present in mitochondria probably induced increased H_2O_2 production rates in striatal mitochondria, as observed in our experimental model. It is already known, that acute paraquat treatment (10.96 mg/Kg) increased oxidative stress levels in neurons of different brain areas (Wu et al. 2013). In our study, DPI inhibited H_2O_2 formation in mitochondria, giving support to the idea of paraquat redox cycling as the main mechanism of H_2O_2 generation.

In this context, it is relevant to discuss the effect of paraquat on striatal mitochondrial membrane potential. In the present study, we observed an increased level of striatal mitochondrial polarization in state 4 condition after acute paraquat treatment. This fact could be due to a transient inhibition of the ATPsynthase, as previously reported by Palmeira and colleagues for in vitro studies in liver (Palmeira et al. 1995). In order to test this hypothesis, we measured mitochondrial membrane potential in the presence of ADP (State 3). The results showed that ADP induced a stronger depolarization in mitochondria from paraquat treated animals as compared with those from untreated rats, indicating that ATP synthase does not seem to be inhibited. In this study the high level of striatum mitochondrial polarization after paraquat treatment was associated with an enhanced H_2O_2 release, in agreement with the reported $\Delta\psi_m$-dependence of ROS generation (Korshunov et al. 1997; Starkov and Fiskum 2003).We could suggest that the shift of $\Delta\psi_m$ towards hyperpolarization after acute paraquat treatment, in agreement with the high oxygen uptake observed in non phosphorylating mitochondrial state, could be related with an impaired mitochondrial calcium homeostasis. It is well known that mitochondrial Ca^{2+} uptake depends on high $\Delta\psi_m$, and that Ca^{2+} itself can also act on $\Delta\psi_m$ shifting it to more negative values. These observations could be the consequence of a transient inhibition of the F_0F_1-ATPase and of the adenine nucleotide translocase. In fact, a diminished activity of the nucleotide translocase and impaired phosphorylation of ADP after paraquat treatment has been reported in brain mitochondria, wich is consistent with the increased $\Delta\psi_m$ and ROS generation observed in this study (Gomez-Puyou et al. 1979; Roman et al. 1981).

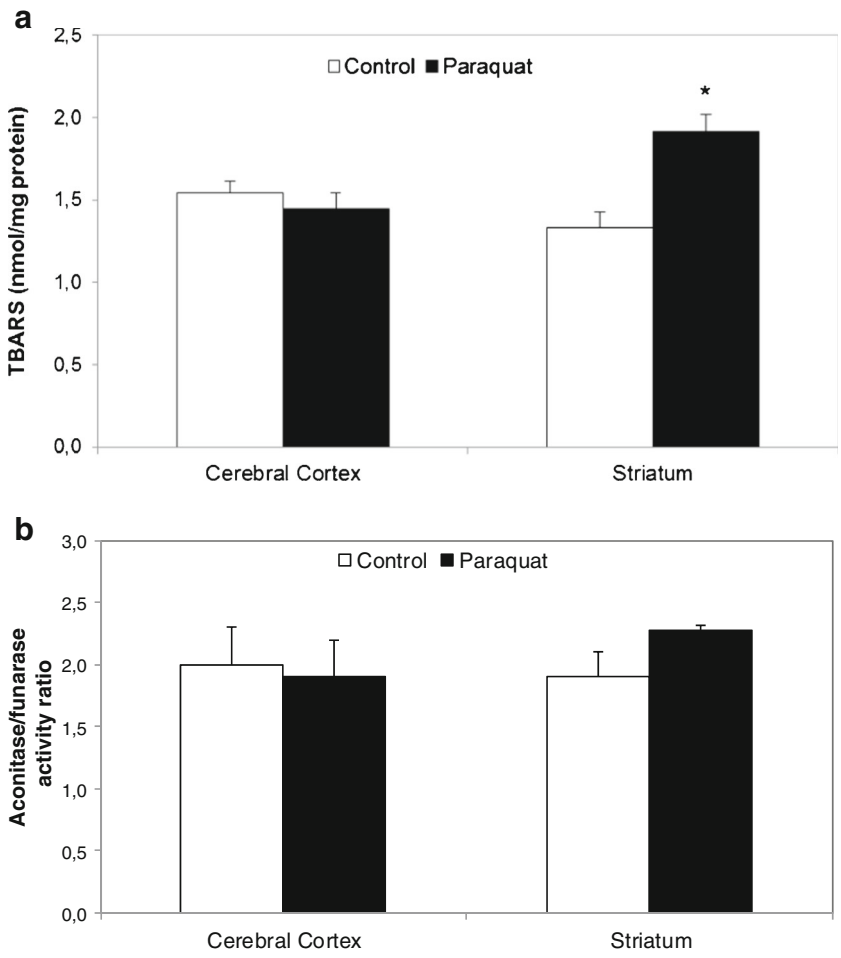

Fig. 6 Acute paraquat treatment effects on TBARS production and aconitase activity. **(a)** *TBARS production.* Bars represent the mean ± SEM of 3 individual mitochondrial samples, each obtained from a pool of cerebral cortex or striatum of 3 rats. (*$p < 0.001$, as compared with control value). **(b)** *Aconitase activity.* Bars represent the aconitase/fumarase activity ratio ± SEM of 4 individual mitochondrial samples, each obtained from a pool of cerebral cortex or striatum of 3 rats

Increased ROS production induced oxidative damage to lipids, proteins and DNA. Alterations in the content and/or composition of cardiolipin have been well documented in a variety of pathological states associated with mitochondrial dysfunction such as ischemia-reperfusion and oxidative stress (Nakahara et al. 1992; Sen et al. 2006). The current study showed an increased cardiolipin oxidation/depletion in striatal intact mitochondria after paraquat treatment. But, no significant changes were observed in cardiolipin oxidation/depletion of striatal mitochondria after antimycin pre-incubation in paraquat-treated animals, indicating that this effect could also be a consequence of paraquat redox cycling reactions. Cardiolipin is required for optimal function of mitochondrial respiratory chain complexes, including Complex I (Paradies et al. 2002) and ATPsynthase (Eble et al. 1990). We suggested that oxidative cardiolipin damage could be involved in the Complex I inhibition induced by paraquat. We also observed significant differences in striatal TBARS production levels between untreated and paraquat-treated animals, supporting the obtained results of changes in NAO fluorescence and increased H_2O_2 production. In this work, the increased production of H_2O_2 and its peroxidative effect observed in striatal mitochondria was not associated with aconitase inhibition.

It is important to mention that no significant changes were observed after paraquat treatment in any of the mitochondrial functionality parameters evaluated in cortical mitochondria, indicating that possibly this brain area could be more resistant to an oxidative stress induced by paraquat in this experimental model. The cause of the striatum vulnerability is not clear, but at least three hypothesis can explain why striatal mitochondria

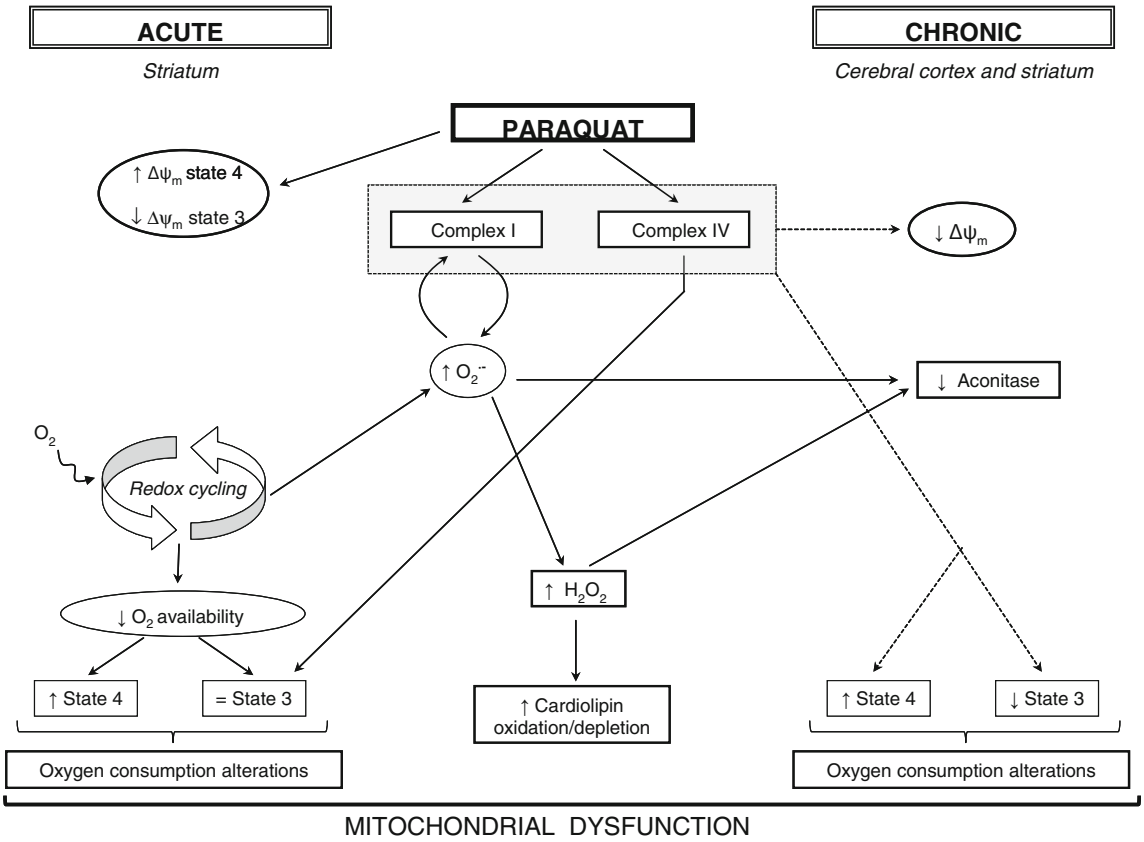

Fig. 7 Acute and chronic paraquat effects on mitochondrial function. Schematic representation of paraquat-induced effects and mechanisms involved after acute or chronic exposure. As described in the *Discussion* section, acute paraquat treatment only impairs striatal mitochondrial function, while chronic treatment also alters cerebral cortex. In the center of the scheme the effects and action mechanisms of paraquat that are shared by both acute and chronic treatments are shown: inhibition of complex I and IV and the increment of cardiolipin oxidation/depletion as a consequence of increased H_2O_2 production. Paraquat redox cycling-induced by **acute** exposure (**left side** of the scheme) decreases O_2 availability leading to mitochondrial oxygen consumption alterations characterized by an increase in respiratory state 4 and no changes in respiratory state 3. In addition, paraquat redox cycling increases superoxide anion levels triggering oxidative stress and important cardiolipin peroxidation. Moreover, acute paraquat treatment induces clear changes in mitochondrial membrane polarization. On the other hand, after **chronic** exposure (**right side** of the scheme) the direct action of paraquat on the respiratory chain that inhibit complex I and complex IV produces an important decrease in membrane potential and a decrease in state 3 respiratory rates, indicating impaired mitochondrial function. Enhanced $O_2^{\bullet-}$ and H_2O_2 production induced by paraquat inhibits aconitase activity after chronic treatment, effect that was not observed after acute treatment. Altogether, despite paraquat induced mitochondrial dysfunction, the brain areas and the mechanisms involved in acute paraquat damage partially differ from those associated to the chronic exposure. Chronic data was taken from (Czerniczyniec et al. 2011; Czerniczyniec et al. 2013). (↓) decrease; (↑) increase; (=) no changes

are more sensitive than cortical mitochondria to paraquat damage: 1) dopapminergic neurons are particular prone to endogenous oxidative metabolism due to high rate of MAO activity, dopamine auto-oxidation, low levels of antioxidants and high iron content, 2) the presence of a higher mitochondrial mass in striatum as compared with hippocampus and cerebral cortex (Pickrell et al. 2011) and 3) the difference in the transport and accumulation of paraquat between brain regions (striatum > frontal cortex > cerebellum) (Prasad et al. 2007).

If the oxidative stress and the mitochondrial dysfunction persisted, induction of different death signaling pathways could appear after paraquat poisoning. The results presented let us suggest that it would be important to apply a pharmacological rescue against brain injury in order to reduce the potential neuronal death events.

Conclusions

In conclusion, in the present work, a clear striatal mitochondrial dysfunction was observed after 24 h of an acute paraquat insult (25 mg/kg *ip*), due to both paraquat redox cycling reactions and to a direct effect on respiratory chain. As a consequence, we observed an impairment of the mitochondrial electron transport, a disturbed $\Delta\Psi_m$ and important oxidative damage to lipids especially to cardiolipin. Brain cortex seemed to be more resistant to paraquat-induced oxidative stress damage in this experimental model.

On the other hand, we could conclude that the mechanisms involved in mitochondrial acute paraquat damage partially differ from those associated to the chronic exposure (Fig. 7) (Czerniczyniec et al. 2011; Czerniczyniec et al. 2013) probably due to the fact that paraquat redox cycling reactions still occur 24 h after acute administration.

Acknowledgments This research was supported by grants from Universidad de Buenos Aires (B025 and 20020100100511) and Consejo Nacional de Investigaciones Científicas y Técnicas (PIP112-200801–00653), Argentina.

Conflict of interest The authors declare that there are no conflicts of interest.

References

Agarwal R, Srinivas R, Aggarwal AN, Gupta D (2006) Experience with paraquat poisoning in a respiratory intensive care unit in North India. Singap Med J 47:1033–1037

Agarwal R, Srinivas R, Aggarwal AN, Gupta D (2007) Immunosuppressive therapy in lung injury due to paraquat poisoning: a meta-analysis. Singap Med J 48:1000–1005

Block K, Gorin Y, Abboud HE (2009) Subcellular localization of Nox4 and regulation in Diabetes. Proc Natl Acad Sci U S A 106:14385–14390

Boveris A (1984) Determination of the production of superoxide radicals and hydrogen peroxide in mitochondria. Methods Enzymol 105: 429–435

Boveris A, Costa LE, Cadenas E, Poderoso JJ (1999) Regulation of mitochondrial respiration by adenosine diphosphate, oxygen, and nitric oxide. Methods Enzymol 301:188–198

Breckenridge CB et al. (2013) Pharmacokinetic, neurochemical, stereological and neuropathological studies on the potential effects of paraquat in the substantia nigra pars compacta and striatum of male C57BL/6 J Mice. Neurotoxicology 37:1–14

Bustamante J, Di Libero E, Fernandez-Cobo M, Monti N, Cadenas E, Boveris A (2004) Kinetic Analysis of Thapsigargin-Induced Thymocyte Apoptosis. Free Radic Biol Med 37:1490–1498

Case AJ, Li S, Basu U, Tian J, Zimmerman MC (2013) Mitochondrial-localized NADPH oxidase 4 is a source of superoxide in angiotensin II-stimulated neurons. Am J Physiol Heart Circ Physiol 305:H19–H28

Czerniczyniec A, Karadayian AG, Bustamante J, Cutrera RA, Lores-arnaiz S (2011) Paraquat induces behavioral changes and cortical and striatal mitochondrial dysfunction. Free Radic Biol Med 51: 1428–1436

Czerniczyniec A, Lores-Arnaiz S, Bustamante J (2013) Mitochondrial susceptibility in a model of paraquat neurotoxicity. Free Radic Res 47:614–623

Dinis-Oliveira RJ, Duarte JA, Sanchez-Navarro A, Remiao F, Bastos ML, Carvalho F (2008) Paraquat poisonings: mechanisms of lung toxicity, clinical features, and treatment. Crit Rev Toxicol 38:13–71

Dinis-Oliveira RJ et al. (2007) Sodium salicylate prevents paraquat-induced apoptosis in the rat lung. Free Radic Biol Med 43:48–61

Eble KS, Coleman WB, Hantgan RR, Cunningham CC (1990) Tightly associated cardiolipin in the bovine heart mitochondrial ATP synthase as analyzed by 31P nuclear magnetic resonance spectroscopy. J Biol Chem 265:19434–19440

Estabrook R (1967) Mitochondrial respiratory control and the polarographic measurement of ADP:O ratios. Methods Enzymol 10:41–47

Esterbauer H, Cheeseman KH, Dianzani MU, Poli G, Slater TF (1982) Separation and characterization of the aldehydic products of lipid peroxidation stimulated by ADP-Fe2+ in rat liver microsomes. Biochem J 208:129–140

Gardner PR (2002) Aconitase: sensitive target and measure of superoxide. Methods Enzymol 349:9–23

Gocgeldi E et al. (2008) Establishing the use of melatonin as an adjuvant therapeutic against paraquat-induced lung toxicity in rats. Exp Biol Med (Maywood) 233:1133–1141

Gomez-Puyou A, Tuena de Gomez-Puyou M, Klapp M, Carafoli E (1979) The effect of calcium on the translocation of adenine nucleotides in rat liver mitochondria. Arch Biochem Biophys 194:399–404

Gram TE (1997) Chemically reactive intermediates and pulmonary xenobiotic Toxicity. Pharmacol Rev 49:297–341

Hatefi Y (1985) The mitochondrial electron transport and oxidative phosphorylation System. Annu Rev Biochem 54:1015–1069

Huang CL et al. (2015) Paraquat Induces Cell Death Through Impairing Mitochondrial Membrane Permeability Mol Neurobiol

Korshunov SS, Skulachev VP, Starkov AA (1997) High protonic potential actuates a mechanism of production of reactive oxygen species in mitochondria. FEBS Lett 416:15–18

Kuroda J, Ago T, Matsushima S, Zhai P, Schneider MD, Sadoshima J (2010) NADPH oxidase 4 (Nox4) is a major source of oxidative stress in the failing heart. Proc Natl Acad Sci U S A 107:15565–15570

Lin C, Yen TH, Juang YY, Lin JL, Lee SH (2014) Psychiatric comorbidity and its impact on mortality in patients who attempted suicide by paraquat poisoning during 2000–2010. PLoS One 9:e112160

Lores-Arnaiz S, Coronel M, Boveris A (1999) Nitric oxide, superoxide and hydrogen peroxide production in brain mitochondria after haloperidol treatment. Nitric Oxide Biol Chem 3:235–243

Lowry OH, Rosebrough NJ, Farr AL, Randall RJ (1951) Protein measurement with the folin phenol reagent. J Biol Chem 193:265–275

Madison DV, Edson EB (2001) Preparation of hippocampal brain slices Curr Protoc Neurosci Chapter 6:Unit 6 4

Mainwaring G et al. (2006) Identification of early molecular pathways affected by paraquat in rat lung. Toxicology 225:157–172

McCormack AL, Thiruchelvam M, Manning-Bog AB, Thiffault C, Langston JW, Cory-Slechta DA, Di Monte DA (2002) Environmental risk factors and parkinson's disease: selective degeneration of nigral dopaminergic neurons caused by the herbicide paraquat. Neurobiol Dis 10:119–127

McMillin JB, Dowhan W (2002) Cardiolipin and apoptosis biochim. Biophys Acta 1585:97–107

Nakahara I et al. (1992) Changes in major phospholipids of mitochondria during postischemic reperfusion in rat brain. J Neurosurg 76:244–250

Nomura K, Imai H, Koumura T, Kobayashi T, Nakagawa Y (2000) Mitochondrial phospholipid hydroperoxide glutathione peroxidase inhibits the release of cytochrome c from mitochondria by suppressing the peroxidation of cardiolipin in hypoglycaemia-induced apoptosis. Biochem J 351:183–193

Onyeama HP, Oehme FW (1984) A literature review of paraquat toxicity. Vet Hum Toxicol 26:494–502

Ossowska K et al. (2005) A slowly developing dysfunction of dopaminergic nigrostriatal neurons induced by long-term paraquat administration in rats: an animal model of preclinical stages of Parkinson's disease? Eur J Neurosci 22:1294–1304

Palmeira CM, Moreno AJ, Madeira VM (1995) Mitochondrial bioenergetics is affected by the herbicide paraquat Biochim Biophys Acta 1229:187–192

Paradies G, Petrosillo G, Pistolese M, Ruggiero FM (2000) The effect of reactive oxygen species generated from the mitochondrial electron transport chain on the cytochrome c oxidase activity and on the cardiolipin content in bovine heart submitochondrial particles. FEBS Lett 466:323–326

Paradies G, Petrosillo G, Pistolese M, Ruggiero FM (2001) Reactive oxygen species generated by the mitochondrial respiratory chain affect the complex iii activity via cardiolipin peroxidation in beef-heart submitochondrial particles. Mitochondrion 1:151–159

Paradies G, Petrosillo G, Pistolese M, Ruggiero FM (2002) Reactive oxygen species affect mitochondrial electron transport complex i activity through oxidative cardiolipin damage. Gene 286:135–141

Paraquat information center on behalf of Syngenta crop protection AG. Global registration status of paraquat (Gramoxone). (2015) Retrieved from http://paraquat.com/safety/regulation. Accessed 20 March 2015).

Petit JM, Maftah A, Ratinaud MH, Julien R (1992) 10 N-nonyl acridine orange interacts with cardiolipin and allows the quantification of this phospholipid in isolated Mitochondria. Eur J Biochem 209:267–273

Pickrell AM, Fukui H, Wang X, Pinto M, Moraes CT (2011) The striatum is highly susceptible to mitochondrial oxidative phosphorylation dysfunctions. J Neurosci 31:9895–9904

Prasad K, Winnik B, Thiruchelvam MJ, Buckley B, Mirochnitchenko O, Richfield EK (2007) Prolonged toxicokinetics and toxicodynamics of paraquat in mouse brain. Environ Health Perspect 115:1448–1453

Roman I, Clark A, Swanson PD (1981) The interaction of calcium transport and adp phosphorylation in brain mitochondria. Membr Biochem 4:1–9

Santos RS et al. (2011) Effects of oleanolic acid on pulmonary morphofunctional and biochemical variables in experimental acute lung Injury. Respir Physiol Neurobiol 179:129–136

Sen T, Sen N, Tripathi G, Chatterjee U, Chakrabarti S (2006) Lipid peroxidation associated cardiolipin loss and membrane depolarization in rat brain mitochondria. Neurochem Int 49:20–27

Senarathna L, Eddleston M, Wilks MF, Woollen BH, Tomenson JA, Roberts DM, Buckley NA (2009) Prediction of outcome after paraquat poisoning by measurement of the plasma paraquat concentration. Qjm 102:251–259

Shimizu K, Matsubara K, Ohtaki K, Fujimaru S, Saito O, Shiono H (2003) Paraquat induces long-lasting dopamine overflow through the excitotoxic pathway in the striatum of freely moving rats. Brain Res 976:243–252

Shimizu K et al. (2001) Carrier-mediated processes in blood–brain barrier penetration and neural uptake of paraquat. Brain Res 906:135–142

Sittipunt C (2005) Paraquat poisoning. Respir Care 50:383–385

Starkov AA, Fiskum G (2003) Regulation of brain mitochondrial H2O2 production by membrane potential and NAD(P)H redox state. J Neurochem 86:1101–1107

Thiruchelvam M, Richfield EK, Baggs RB, Tank AW, Cory-slechta DA (2000) The nigrostriatal dopaminergic system as a preferential target of repeated exposures to combined paraquat and maneb: implications for parkinson's disease. J Neurosci 20:9207–9214

Wesseling C, van Wendel de Joode B, Ruepert C, Leon C, Monge P, Hermosillo H, Partanen TJ (2001) Paraquat in Developing countries. Int J Occup Environ Health 7:275–286

Wright MM, Howe AG, Zaremberg V (2004) Cell membranes and apoptosis: role of cardiolipin, phosphatidylcholine, and anticancer lipid Analogues. Biochem Cell Biol 82:18–26

Wu B, Song B, Yang H, Huang B, Chi B, Guo Y, Liu H (2013) Central nervous system damage due to acute paraquat poisoning: an experimental study with rat. Model Neurotoxicology 35C:62–70